# Plane Wave Excitation for Frequency Domain Electromagnetic Problems by Means of Impedance Boundary Condition

Silvano Chialina[1], Matteo Cicuttin[2], Lorenzo Codecasa[3], Ruben Specogna[2], and Francesco Trevisan[2]

[1]Emilab s.r.l., Amaro I-33020, Italy
[2]Dipartimento di Ingegneria Elettrica, Gestionale e Meccanica, Università di Udine, Udine I-33100, Italy
[3]Dipartimento di Elettronica, Informazione e Bioingegneria, Politecnico di Milano, Milan I-20133, Italy

**This paper presents how a plane wave excitation could be modeled in the context of the discrete geometric approach (DGA) by means of an impedance boundary condition, a capability that DGA was lacking. A methodology for the construction of an equivalent model of an anechoic wall is then presented as an application of the developed theory. The advantages of the resulting model are twofold: considering all the geometric details of the anechoic material requires more computational resources; in addition when an entire anechoic chamber is to be modeled, it is easier to deal with a flat wall rather than one covered with cones and ferrite tiles. The proposed equivalent model allows for a great simplification, while maintaining a good degree of accuracy.**

*Index Terms*— **Anechoic wall, discrete geometric approach (DGA), impedance boundary condition, plane wave excitation.**

## I. Introduction

THE aim of this paper is to formulate an impedance boundary condition with plane wave excitation (excitation condition, for conciseness) for the discrete geometric approach (DGA), a numerical method useful to solve a wide class of problems, in particular the full electromagnetic wave propagation problem [1]. The proposed boundary condition allows to apply a plane wave excitation to the simulation domain boundaries, but also permits to the reflected waves to exit. An application of the condition aimed at the construction of an equivalent electromagnetic model of a real anechoic wall is then presented, since numerical modeling of anechoic chambers is a very actual topic [4], [5].

An anechoic wall is composed by a number of basic elements which we call unitary cells (Fig. 1). A cell consists of four distinct regions: from left to right, the first one represents the air in front of the wall, the second accommodates the absorbing cones, the third is air again, and the fourth is where the ferrite tiles are placed. The leftmost surface $\Sigma$ represents the excitation, where a plane wave of angular frequency $\omega$ and wave vector normal to $\Sigma$ is forced. The study of an entire wall reduces essentially to the study of that unitary cell, which is also the computational domain $\Omega$ where the numerical problem is defined. Then, the wave impedance is calculated on a plane $\Pi$ (Fig. 3) parallel to $\Sigma$ internal to $\Omega$ and not intersecting the cone region. Finally, using standard formulas from transmission line theory, the impedance $Z_\Pi$ calculated on $\Pi$ is de-embedded to the right side of the unitary cell (Fig. 4), obtaining $Z_{\Pi'}$. In this way, the original model with cone-ferrite assembly can be replaced by an equivalent one made of an empty volume terminated with the de-embedded impedance $Z_{\Pi'}$. Such an equivalent model will enable us to simulate an entire anechoic wall and not just an unitary cell, with quite good accuracy, reduced computational effort, and ease of modeling, since the required number of mesh elements is much smaller and only flat surfaces are involved.

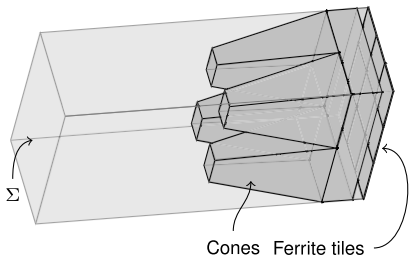


Fig. 1. Unitary cell, which consists of the excitation $\Sigma$, air (light gray), cones (dark gray), and ferrites (surface at the right).

This paper starts with a brief review of the continuous wave propagation problem, together with its discrete counterpart; in addition, the admittance boundary conditions of [1] are recalled, both in the continuous and discrete setting. In Section IV, this paper goes through the details behind the impedance boundary condition with excitation. Finally, the application is described and numerical results are presented.

## II. Electromagnetic Problem

The electromagnetic wave propagation problem in the frequency domain at angular frequency $\omega$ is obtained directly from Maxwell's equations

$$\nabla \times \boldsymbol{e}(\boldsymbol{r}) = -i\omega \boldsymbol{b}(\boldsymbol{r}) \tag{1}$$

$$\nabla \times \boldsymbol{h}(\boldsymbol{r}) = i\omega \boldsymbol{d}(\boldsymbol{r}) + \boldsymbol{j}_s(\boldsymbol{r}) \tag{2}$$

together with the constitutive relations

$$\boldsymbol{d}(\boldsymbol{r}) = \boldsymbol{\epsilon}(\boldsymbol{r})\boldsymbol{e}(\boldsymbol{r}) \tag{3}$$

$$\boldsymbol{h}(\boldsymbol{r}) = \boldsymbol{\nu}(\boldsymbol{r})\boldsymbol{b}(\boldsymbol{r}) \tag{4}$$

where $\boldsymbol{d}$, $\boldsymbol{e}$, $\boldsymbol{h}$, and $\boldsymbol{b}$ are complex-valued vector functions of the position vector $\boldsymbol{r} \in \Omega$, representing, respectively,

Manuscript received May 23, 2014; revised September 8, 2014; accepted September 12, 2014. Date of current version April 22, 2015. Corresponding author: M. Cicuttin (e-mail: matteo.cicuttin@uniud.it).

Color versions of one or more of the figures in this paper are available online at http://ieeexplore.ieee.org.

Digital Object Identifier 10.1109/TMAG.2014.2358701

electric displacement, electric, magnetic, and magnetic induction fields; $\boldsymbol{\epsilon}$ and $\boldsymbol{\nu}$ are, respectively, the electric and magnetic material positive definite tensors. For the sake of clarity and conciseness, the position dependence of functions $\boldsymbol{d}$, $\boldsymbol{e}$, $\boldsymbol{h}$, $\boldsymbol{b}$, $\boldsymbol{j}_s$, $\boldsymbol{\nu}$, and $\boldsymbol{\epsilon}$ will be considered implicit from now on and thus omitted. By neglecting the imposed currents $\boldsymbol{j}_s$ and substituting (3) and (4) in (2), and then using (1), the electromagnetic wave propagation problem becomes

$$\nabla \times (\boldsymbol{\nu} \nabla \times \boldsymbol{e}) - \omega^2 \boldsymbol{\epsilon} \boldsymbol{e} = \mathbf{0} \tag{5}$$

which can be solved subject to specific boundary conditions, for example the impedance boundary condition

$$Z \boldsymbol{h} \times \boldsymbol{n} = ((\boldsymbol{n} \times \boldsymbol{e}) \times \boldsymbol{n}) \tag{6}$$

where $\boldsymbol{n}$ is the outward normal of the considered boundary surface $\partial\Omega$. From now we will develop our discussion using mainly admittance instead of impedance, because it arises naturally from the proposed formulation.

## III. DGA Formulation of the Electromagnetic Problem

The DGA requires a discretization of the region $\Omega$ in which the problem is defined, consisting in a pair of interlocked grids $\mathcal{G}$ and $\tilde{\mathcal{G}}$. The grid $\mathcal{G}$ is tetrahedral, while $\tilde{\mathcal{G}}$ is obtained from $\mathcal{G}$ by barycentric sub-division [2]. The electromagnetic quantities are defined on the geometric elements composing these grids, in particular:

1) the electromotive force $U_i = \int_{e_i} \boldsymbol{e} \cdot d\boldsymbol{l}$ on the primal edges $e_i \in \mathcal{G}$;
2) the magnetic flux $\Phi_i = \int_{f_i} \boldsymbol{b} \cdot d\boldsymbol{s}$ on the primal faces $f_i \in \mathcal{G}$;
3) the magnetomotive force $F_i = \int_{\tilde{e}_i} \boldsymbol{h} \cdot d\boldsymbol{l}$, on the dual edges $\tilde{e}_i \in \tilde{\mathcal{G}}$;
4) the electric flux $\Psi_i = \int_{\tilde{f}_i} \boldsymbol{d} \cdot d\boldsymbol{s}$, on the dual faces $\tilde{f}_i \in \tilde{\mathcal{G}}$.

In addition, the standard face-edge incidence matrices $\mathbf{C}$ on $\mathcal{G}$ and $\mathbf{C}^T$ on $\tilde{\mathcal{G}}$ are introduced. According to the DGA, (1)–(4) have their discrete counterparts, written in terms of the quantities defined previously

$$\mathbf{C}\mathbf{U} = -i\omega\boldsymbol{\Phi} \tag{7}$$

$$\mathbf{C}^T\mathbf{F} = i\omega\boldsymbol{\Psi} + \mathbf{I}_s \tag{8}$$

$$\boldsymbol{\Psi} = \mathbf{M}_\epsilon \mathbf{U} \tag{9}$$

$$\mathbf{F} = \mathbf{M}_\nu \boldsymbol{\Phi}. \tag{10}$$

The arrays $\mathbf{U}$, $\boldsymbol{\Phi}$, $\mathbf{F}$, and $\boldsymbol{\Psi}$ collect circulations and fluxes of the electromagnetic quantities on edges and faces of a given tetrahedron, while symmetric positive definite matrices $\mathbf{M}_\epsilon$ and $\mathbf{M}_\nu$ are calculated according to [2]. The array $\mathbf{I}_s$ denotes the conduction current across dual faces but, as in the continuous case, they are not considered in the following. The discrete wave propagation problem is then derived as

$$\left(\mathbf{C}^T\mathbf{M}_\nu\mathbf{C} - \omega^2\mathbf{M}_\epsilon\right)\mathbf{U} = \mathbf{0}. \tag{11}$$

The discrete counterpart of the admittance boundary conditions is encoded as

$$\mathbf{F}^b = \mathbf{M}_Y \mathbf{U} \tag{12}$$

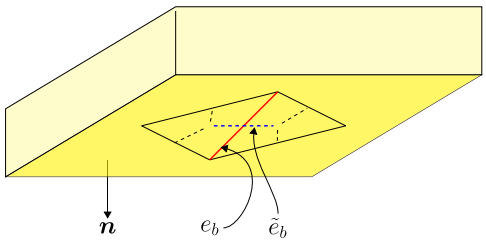


Fig. 2. Portion of $\partial\Omega$ is shown, together with primal boundary edge $e_b$ in one to one correspondence with a dual boundary edge $\tilde{e}_b$.

where the array $\mathbf{F}^b$ has the same number of elements of $\mathbf{U}$, but its non-zero entries are only the ones associated to dual boundary edges $\tilde{e}_b$ of $\partial\Omega$, which are in one to one correspondence to primal boundary edges $e_b$ (Fig. 2).

The matrix $\mathbf{M}_Y$ has also non-zero entries only in correspondence of the boundary edges. Its entries are calculated from the admittance parameter $Y$, as described in [1]. According to [1], condition (12) is integrated into (11) as

$$\left(\mathbf{C}^T\mathbf{M}_\nu\mathbf{C} - \omega^2\mathbf{M}_\epsilon\right)\mathbf{U} + i\omega\mathbf{F}^b = \mathbf{0}. \tag{13}$$

## IV. Impedance Boundary Condition With Plane Wave Excitation

The goal of the presented boundary condition is to apply a plane wave entering the domain $\Omega$ through a specific portion $\Sigma$ of the boundary $\partial\Omega$. Since in $\Omega$ there could be reflections and scattering phenomena that must be considered, we can split the electromagnetic field across $\Sigma$ in two separate components:

1) the component entering $\Sigma$, due to the imposed excitation and given by the fields $\boldsymbol{e}^-$, $\boldsymbol{h}^-$, and directed toward $-\boldsymbol{n}$;
2) the component exiting $\Sigma$, given by $\boldsymbol{e}^+$, $\boldsymbol{h}^+$ due to the reflections, directed toward $\boldsymbol{n}$.

Between the pair of fields on $\Sigma$

$$\boldsymbol{e} = \boldsymbol{e}^+ + \boldsymbol{e}^- \tag{14}$$

$$\boldsymbol{h} = \boldsymbol{h}^+ + \boldsymbol{h}^- \tag{15}$$

hold according to (6). The excitation $\Sigma$ is characterized by a given wave admittance $Y$ with respect to the normal direction $\boldsymbol{n}$, where

$$\boldsymbol{h}^+ \times \boldsymbol{n} = Y((\boldsymbol{n} \times \boldsymbol{e}^+) \times \boldsymbol{n}) \tag{16}$$

$$\boldsymbol{h}^- \times \boldsymbol{n} = -Y((\boldsymbol{n} \times \boldsymbol{e}^-) \times \boldsymbol{n}) \tag{17}$$

hold. The fact that the wave vector direction is exactly $\boldsymbol{n}$ has important consequences, as it will be explained below. In the following two sections it will be shown how, from the considerations made, admittance boundary conditions with excitation are incorporated in the problem (13).

### A. Tangent Electric Field Exiting $\Omega$

The left hand side of (16) can be rewritten decomposing $\boldsymbol{h}^+$ in its normal component $\boldsymbol{h}_n^+$ and in its tangential component $\boldsymbol{h}_t^+$

$$\boldsymbol{h}^+ \times \boldsymbol{n} = \left(\boldsymbol{h}_n^+ + \boldsymbol{h}_t^+\right) \times \boldsymbol{n} = \boldsymbol{h}_t^+ \times \boldsymbol{n} \tag{18}$$

and (16) becomes

$$\boldsymbol{h}_t^+ \times \boldsymbol{n} = Y \boldsymbol{e}_t^+. \tag{19}$$

This last formula establishes a relation between the tangential components of the electric and magnetic fields exiting $\Omega$: they are proportional to each other by the factor $Y$, the wave admittance of $\Sigma$. The direct implication is that only waves exiting $\Omega$ with normal incidence will experience no reflection.

According to (12), boundary condition for the exiting component of the field are written as

$$\mathbf{F}^{b^+} = \mathbf{M}_Y \mathbf{U}^+ \tag{20}$$

where $\mathbf{F}^{b^+}$ and $\mathbf{U}^+$ are the magnetomotive and electromotive forces due to the exiting wave. In addition, $\mathbf{M}_Y$ satisfies (20) exactly when the tangential components of the electric field are piecewise uniform on each element of $\Sigma$.

### *B. Tangent Electric Field Entering $\Omega$*

A similar reasoning can be carried out for the field component entering $\Omega$. In this case (17) is considered, yielding

$$\boldsymbol{h}_t^- \times \boldsymbol{n} = -Y \boldsymbol{e}_t^-. \tag{21}$$

Again, (21) can be directly translated in discrete form

$$\mathbf{F}^{b^-} = -\mathbf{M}_Y \mathbf{U}^- \tag{22}$$

where $\mathbf{F}^{b^-}$ and $\mathbf{U}^-$ are the magnetomotive and electromotive forces due to the entering wave. This second equation, as shown below, involves known quantities and is used to impose the excitation on $\Sigma$. Again, it relates exactly the tangential components of the electric and magnetic fields, so it permits to apply a plane wave with normal incidence to $\Sigma$.

### *C. Obtaining the Linear System*

Since the fields are decomposed in entering and exiting components, it holds that

$$\mathbf{F}^b = \mathbf{F}^{b^+} + \mathbf{F}^{b^-} \tag{23}$$

$$\mathbf{U} = \mathbf{U}^+ + \mathbf{U}^-. \tag{24}$$

The array $\mathbf{U}$ is formed by two contributes. The electromotive force due to the imposed excitation, which is fully known, is expressed by $\mathbf{U}^-$ and is non-zero only in correspondence of the entries of the primal boundary edges of $\Sigma$. The array $\mathbf{U}^+$, on the other hand, is unknown and in correspondence of the primal edges of $\Sigma$ it accounts for the electromotive force due to the wave exiting $\Omega$. Starting from (23) and using (20) and (24), excitation boundary condition is deduced

$$\begin{aligned}\mathbf{F}^b &= \mathbf{F}^{b^+} + \mathbf{F}^{b^-} = \mathbf{M}_Y \mathbf{U}^+ + \mathbf{F}^{b^-} \\ &= \mathbf{M}_Y (\mathbf{U} - \mathbf{U}^-) + \mathbf{F}^{b^-} \\ &= \mathbf{M}_Y \mathbf{U} + 2\mathbf{F}^{b^-}.\end{aligned} \tag{25}$$

Finally, by substituting $\mathbf{F}^b$ from (25) in (13) we obtain

$$\left(\mathbf{C}^T \mathbf{M}_\nu \mathbf{C} - \omega^2 \mathbf{M}_\epsilon\right)\mathbf{U} + i\omega \mathbf{M}_Y \mathbf{U} = -2i\omega \mathbf{F}^{b^-} \tag{26}$$

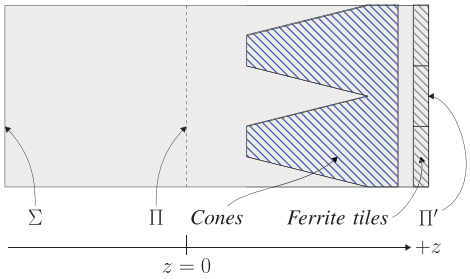


Fig. 3. Sectional view of the cone-ferrite assembly (not to scale). Excitation $\Sigma$, the impedance calculation plane $\Pi$ and impedance de-embedding plane $\Pi'$ are indicated.

which allows to apply a magnetic field excitation, computing the entries $F_i^{b^-}$ of $\mathbf{F}^{b^-}$ as

$$F_i^{b^-} = \int_{\tilde{e}_{b_i}} \boldsymbol{h}^- \cdot d\boldsymbol{l} \tag{27}$$

where $\tilde{e}_{b_i}$ are the auxiliary dual edges of $\Sigma$. Otherwise, if an electric field excitation is wanted, (22) can be used to obtain

$$\left(\mathbf{C}^T \mathbf{M}_\nu \mathbf{C} - \omega^2 \mathbf{M}_\epsilon\right)\mathbf{U} + i\omega \mathbf{M}_Y \mathbf{U} = 2i\omega \mathbf{M}_Y \mathbf{U}^- \tag{28}$$

and computing the entries $U_i^{b^-}$ of $\mathbf{U}^-$ as

$$U_i^{b^-} = \int_{e_{b_i}} \boldsymbol{e}^- \cdot d\boldsymbol{l} \tag{29}$$

where $e_{b_i}$ are the primal edges of $\Sigma$.

## V. Equivalent Model

The original model of the unitary cell represents the cone-ferrite assembly in full detail. Material parameters of ferrites and cones were obtained from vendor data sheets. Such detailed modeling requires a very fine discretization that implies the need of more computing and memory resources. For this reason, when a full anechoic chamber has to be simulated, the number of elements could become prohibitive, so a simplified model is wanted.

### *A. Wave Impedance Calculation*

Once the problem (26) is solved, wave impedance can be calculated everywhere in $\Omega$. In our application, it is calculated on a plane $\Pi$ placed at $z = 0$, parallel to the boundary wall (Fig. 3). A grid of $20 \times 20$ points was defined on the plane $\Pi$ and then the tetrahedrons containing these points were identified. For each tetrahedron $T_1, \ldots, T_n$ wave impedance values $Z_1, \ldots, Z_n$ were calculated. Finally, wave impedance on $\Pi$ is obtained from

$$Z_\Pi = \frac{1}{n} \sum_{i=1}^{n} Z_n \tag{30}$$

where the average is performed for numerical robustness reasons.

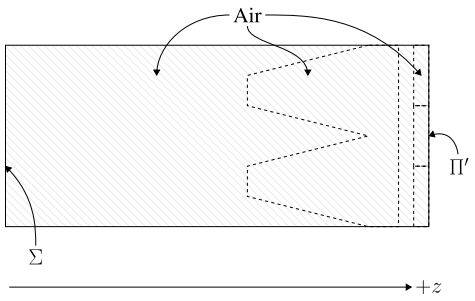


Fig. 4. Sectional view of the equivalent model (not to scale). Whole volume of the equivalent cell is made of air and the de-embedded impedance condition is applied on the plane $\Pi'$.

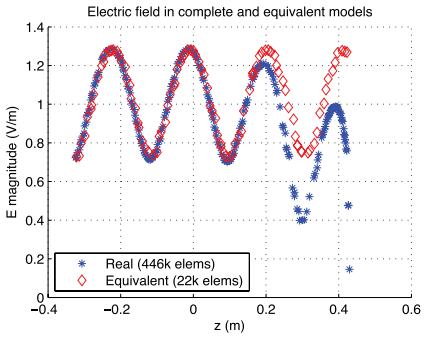


Fig. 5. Electric field comparison between full and equivalent model.

### B. Equivalent Wall Model

The calculated impedance $Z_\Pi$ must now be de-embedded to the boundary $\Pi'$ at the back of the ferrite tiles (Fig. 4), obtaining a new impedance $Z_{\Pi'}$. Impedance $Z_{\Pi'}$ is calculated using a standard formula from transmission line theory [3]

$$Z_{\Pi'}(z) = Z_c \frac{Z_\Pi - iZ_c \tan(\beta z)}{Z_c - iZ_\Pi \tan(\beta z)} \tag{31}$$

where $Z_c = \sqrt{\mu/\epsilon}$ is the characteristic impedance of the space where the wave propagates. $Z_{\Pi'}(z)$ is a function of $z$, the distance of $\Pi'$ from $\Pi$.

## VI. Numerical Results

Two models of the unitary cell were developed, one with full details and one composed entirely by air and terminated by an impedance calculated as in (31). Simulation was performed on the first model, imposing a plane wave excitation on $\Sigma$ with an incident electric field of 1 V/m. Then, wave impedance was calculated on the plane $\Pi$, sampling $\Pi$ on 400 evenly spaced points distributed on a $20 \times 20$ grid. Impedance $Z_{\Pi'}$ was then calculated according to (31) and used as boundary condition on the simplified model. Finally, the excitation condition was used again to impose a plane wave with the same characteristics of the previous experiment on the boundary $\Sigma$ of the simplified model. Numerical results (Figs. 5 and 6) confirm the good quality of the equivalent simplified model since the error was below 5% in most of the zone of interest, despite the drastic reduction (20 times) of the number of elements.

Experiments were made with EMT, a new, general purpose DGA workbench written in C++11. Simulations were performed on OS X 10.9.2 running on a Core i7 3615QM with 16 GB of RAM, Clang/LLVM 3.4 compiler and MKL PARDISO solver. The full model mesh included about 446 000 tetrahedrons, which gave rise to a problem of 485 572 unknowns. Assembly took 8.34 s, while the solver took 55.22 s. The simplified model consisted of about 22 000 tetrahedrons, which gave rise to a problem of 26 624 unknowns: assembly time was 0.45 s while the solver took 0.48 s.

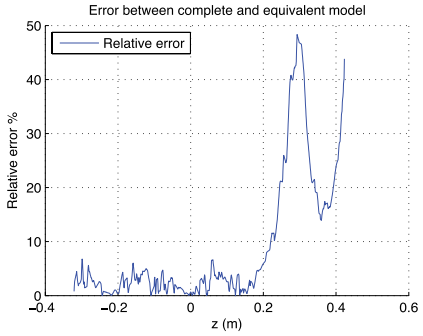


Fig. 6. Percent relative error made by the equivalent model compared with the full one.

## VII. Conclusion

A novel admittance boundary condition with plane wave excitation was developed for the DGA. The new tool was used to study a piece of an anechoic wall in full detail, with the goal of obtaining an equivalent model of the real anechoic wall. In the context of the DGA, the developed boundary condition is a wide generalization of the wave propagation problem since it collects in a single equation a number of other important boundary conditions, namely:

1) admittance boundary condition as in [1], when $\mathbf{F}^{b^-} = \mathbf{0}$;
2) perfect magnetic conductor, when $\mathbf{M}_Y = \mathbf{0}$, $\mathbf{F}^{b^-} = \mathbf{0}$;
3) perfect electric conductor, when $\mathbf{M}_Y = \mathbf{0}$, $\mathbf{F}^{b^-} = \mathbf{0}$, $\mathbf{C}^T\mathbf{M}_\nu\mathbf{C} = \mathbf{0}$, and $\omega^2\mathbf{M}_\epsilon = \mathbf{0}$.

## Acknowledgment

This work was supported in part by EmiLab s.r.l., Amaro, Italy, and in part by the PAR FSC 2013 EMCY Project, Friuli Venezia Giulia Region, Italy. The authors would like to thank Prof. J. Pavo and Dr. T. Benko for the helpful discussions on the unit cell modeling.

## References

[1] L. Codecasa, R. Specogna, and F. Trevisan, "Discrete geometric formulation of admittance boundary conditions for frequency domain problems over tetrahedral dual grids," *IEEE Trans. Antennas Propag.*, vol. 60, no. 8, pp. 3998–4002, Aug. 2012.

[2] L. Codecasa, R. Specogna, and F. Trevisan, "Symmetric positive-definite constitutive matrices for discrete eddy-current problems," *IEEE Trans. Magn.*, vol. 43, no. 2, pp. 510–515, Feb. 2007.

[3] R. E. Collin, *Foundations for Microwave Engineering*. New York, NY, USA: McGraw-Hill, 2000.

[4] I. Munteanu and R. Kakerow, "Simulation methodology for the assessment of field uniformity in a large anechoic chamber," *IEEE Trans. Magn.*, vol. 50, no. 2, Feb. 2014, Art. ID 7005104.

[5] C. Jiakui and W. Yinghong, "Simulation of the field uniformity of anechoic chamber," in *Proc. Int. Symp. Microw., Antenna, Propag. EMC Technol. Wireless Commun.*, Aug. 2007, pp. 1349–1352.